Chapter 4: Centrifuge modelling

4.1 Why centrifuge modelling?

Earthquakes in the past have shown up shortcomings of the current design methodologies and of construction errors at the cost of structural failure and of loss of life. This has progressively led to improvement in analysis, design and construction practices. In this context, Newmark and Rosenbluth (1971) remarked,

"*Earthquake effects on structures systematically bring out the mistakes made in the design and construction even the minutest amount*".

Thus, before applying any earthquake resistant design method to practical problems, or establishing a proposed mechanism, it is better to seek verification from all possible angles. Obtaining physical data on the performance of the design method is essential to that verification. Such physical data could be acquired from detailed case histories during earthquakes but only by putting society at risk in the meantime. The fact that large earthquakes are not frequent and not many piled structures are instrumented makes this method of verification difficult. Therefore, there is a need for small scale physical modelling.

Figure 1.2(c) shows piled tanks at Kobe, which tilted towards the quay wall during the 1995 Kobe earthquake. As earthquakes are very rapid events and as much of the damage to piles occurs beneath the ground, it is hard to ascertain the failure mechanism unless deep excavation is carried out. Physical modelling is one of the alternative techniques to understand such a mechanism. Dynamic centrifuge modelling, a type of physical modelling, has been established as a powerful technique over the past decade in obtaining physical data under earthquake events, and investigating seismic soil-structure interaction problems with one of its aims being verification of mechanisms and design methods.

In order to verify the proposed hypothesis of pile failure described in section 3.5, centrifuge modelling was thought to be most appropriate.

4.1.1 Aims of the centrifuge testing

The central aim of the centrifuge tests is to verify whether fully embedded end-bearing piles passing through saturated, loose to medium dense sands and resting on hard layers, buckle under the action of axial load alone if the surrounding soil liquefies in an earthquake. This can be accomplished by designing the centrifuge experiments in level ground to avoid the effects of lateral spreading. Furthermore, the earthquake should only liquefy the soil and provide no inertia force to the superstructure. This would verify the proposed hypothesis of pile failure mentioned in the section 3.5.

During earthquakes, the predominant loads acting on a pile are axial, inertial and lateral due to movement of the soil (lateral spreading). The failure of a pile can be due to any of these load effects or a suitable combination of them. As mentioned earlier, this research started without making any presumption that lateral spreading is the cause of failure and hence all experiments were designed in level ground. The other aspect of the centrifuge tests was to decouple the effects of axial and inertial load and study the various behaviours of pile foundations during seismic liquefaction.

4.1.2 Contents of the chapter

This chapter discusses the principles of centrifuge modelling, centrifuge facilities at Cambridge University and the test procedure adopted. The methodology used to de-couple the effects of inertia and axial load is also described. Buckling being the proposed hypothesis to be verified, the selection of an appropriate material for the model pile is quite crucial; therefore the development of the model pile is discussed. The tests for structural characterisation of model piles i.e. buckling load tests or plastic moment capacity (M_p) tests are also described. A parallel has been drawn between prototype model piles and an equivalent real concrete pile.

4.2 Principles of centrifuge modelling

In geotechnical engineering, model tests using small size models (1:N where N is the scaling ratio) under 1-g conditions cannot reproduce the prototype behaviour because the stress level due to self-weight is much lower than that in the field scale prototype. The behaviour of soils has been established to be highly non-linear and hence true prototype behaviour can only be observed in a model under stress and strain conditions similar to the prototype. A geotechnical centrifuge enables us to recreate the same stress and strain level within the scaled model by testing a 1:N scale model at N times earth's gravity, created by centrifugal force.

In the centrifuge, the linear dimensions are modelled by a factor 1/N and the stress is modelled by a factor of unity. Scaling laws for many parameters in the model can be obtained by simple dimensional analysis, and are discussed by Schofield (1980 & 1981) as summarised in Table 4.1.

Table 4. 1 Scaling laws

Parameter	**Model/prototype**	**Dimensions**
Length	1/N	L
Mass	$1/N^3$	M
Stress	1	$ML^{-1}T^{-2}$
Strain	1	1
Force	$1/N^2$	MLT^{-2}
Seepage velocity	N	LT^{-1}
Time (seepage)	$1/N^2$	T
Time (dynamic)	1/N	T
Frequency	N	1/T
Acceleration	N	LT^{-2}
Velocity	1	LT^{-1}
EI (bending stiffness)	$1/N^4$	ML^3T^{-2}
M_p (Plastic moment capacity)	$1/N^3$	ML^2T^{-2}

4.3 Dynamic centrifuge modelling

In modelling earthquakes in the centrifuge, lateral acceleration is to be imparted to the model at an appropriate g level. Following the scaling laws in Table 4.1, the scaling factor for acceleration is N and thus, to model earthquakes on a centrifuge, the input acceleration needs to be N times than that of the prototype.

Table 4.1 also shows that the dynamic events occur N times faster than the prototype. Thus in an earthquake test, the rate of pore pressure generation in the model will be N times faster than that in the prototype. Following the scaling law of seepage time, the rate of dissipation of pore pressure in the model is N^2 times faster. If the same soil and pore fluid are used in the model and the prototype there can be a disparity in the observed results, which may lead to wrong conclusions. This anomaly can be avoided by increasing the viscosity of the pore fluid by a factor N in the model. In Cambridge, silicone oil having viscosity N times that of water is used as pore fluid.

4.4 Centrifuge facilities at Cambridge University

The Schofield centre (S.C) at the University of Cambridge houses five centrifuges. They are a 10m diameter balanced beam centrifuge, a 2m diameter drum centrifuge, a 0.8m diameter mini-drum centrifuge, a Mistral bench centrifuge and a sugar centrifuge. For dynamic centrifuge modelling the beam centrifuge is used. The equipments used for the research are described below.

4.4.1 10 m beam centrifuge at Schofield centre

A full description of the 10m balanced-beam centrifuge at the Schofield centre can be found in Schofield (1980). The machine basically consists of a 10m diameter rotating arm that carries models at a working radius of 4.125m. It is capable of accelerating a package with a maximum weight of 900 Kg to a maximum acceleration of 150-g (rotational speed 186 rpm). The beam centrifuge always operates with a balanced counterweight on one swinging platform and a model package on the other. The centrifuge model is normally prepared outside the centrifuge pit, then transferred to a swinging platform and mounted on the beam centrifuge using a crane. Swinging platforms swing outwards and upwards as the centrifuge arm gains speed, so that the direction of the resultant acceleration field passes through the pivot and the centroid of the package. To obtain data, miniature instruments are used within the model. The most common form of instruments that are used at S.C are listed in Table 4.2. A brief description of the instruments used in the centrifuge test is given in the next section.

Table - 4.2 Instruments used at SCC and their functions

Name of the instruments	Functions
Pore pressure transducers (PPT)	To measure pore pressure
Accelerometers	To measure accelerations in dynamic tests
LVDT (Linearly varying differential transformers)	To measure displacements (contact device)
Lasers	To measure displacements (non-contact device)
Strain Gauge	To measure strain in model structure
Load Cells	To measure loads/forces
Pressure transducers	To measure pressure

Video cameras mounted close to the axis of the centrifuge enable visual monitoring of the model to be carried out during a test. Data from the instruments within the package is transferred via a junction box to a computer in the control room through data acquisition software. Data acquisition software is a piece of software that collects the data as recorded from the instruments, digitises it (analog-digital conversion) and transfers this digitised signals through the slips-rings into a specified spot on the hard disk in the control room. CDAQS, Global lab, Daisy lab, Labtech are the software used at SCC. In a dynamic test using CDAQS the signal logging frequency could be as high as 4 kHz per channel. In a recent dynamic centrifuge test data was logged at 40kHz per channel using Daisy lab software and a computer-on-board in the centrifuge. Innovations are currently underway to further boost this logging frequency even higher.

4.4.2 SAM Actuator

Lateral shaking of the model container in flight is achieved using the Stored Angular Momentum (SAM) actuator explained by Madabhushi et al. (1998). This actuator stores energy in a pair of spinning flywheels, releasing the energy to the package by means of a fast acting clutch. The reciprocating motion from the flywheels is converted to lateral shaking by means of a bell-crank mechanism with a variable lever arm length. Adjustment of this lever arm allows the strength of the earthquake to be selected. This actuator allows earthquake frequency, magnitude and duration to be selected by the user. The actuator is shown in Figure 4.1.

Figure: 4.1: SAM actuator at SCC.

4.4.3 ESB Box

Most structures rest on laterally unbounded soil (semi-infinite half-space). To model this boundary condition of the soil, the model container resting in the SAM actuator should cause stress and strain in the model soil identical to that in the prototype. This may be achieved by matching the dynamic stiffness of the soil layer with that of end wall of the model container and is known as ESB box (Equivalent Shear Beam box). In the design of such a box, the column of

soil is idealised as a shear beam whose stiffness varies with depth and the shear deformations in the soil are matched to the shear deformation of the end walls in a step-wise linear fashion. Schofield and Zeng (1992) explain the boundary conditions to be met for a model container as below.

1. The boundary must have the same dynamic stiffness as the adjacent soil to minimise energy reflection in the form of pressure waves.
2. The boundary must have the same friction as the adjacent soil to sustain complementary shear stresses.
3. The sidewalls should be frictionless to have plane strain condition.
4. The model container must have infinite lateral stiffness during the centrifuge spin-up so that a zero lateral strain (K_0) condition can be maintained.
5. The frictional end walls must have the same vertical settlement as the soil layer so that no additional stresses are induced.

The model container used for the centrifuge tests has an internal dimensions of 560mm × 235mm × 220mm and is made up of five rectangular aluminium alloy (dural) rings and rubber sandwiched together with adhesive. This box was designed to operate only at 50-g and at this particular g level the stiffness of the sand layer matches the stiffness of the end walls. This is shown in Figure 4.2. This box was used in carrying out the centrifuge tests.

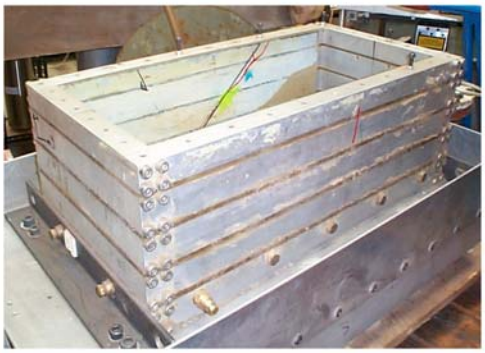

Figure 4.2: ESB box used in the tests.

4.4.4 Pore Pressure Transducer (PPT)

Miniature 7-bar PDCR81 pore pressure transducers manufactured by Druck Ltd. were used to measure the response of excess and hydrostatic pore pressures throughout the test. These transducers contain a flexible silicon diaphragm, protected from the surrounding sand by fitting a

porous sintered bronze cap to the transducer. The typical calibration constants for these PPT's are either 40 kPa/Volt or 80 kPa/volt. A schematic diagram is shown in Figure 4.3.

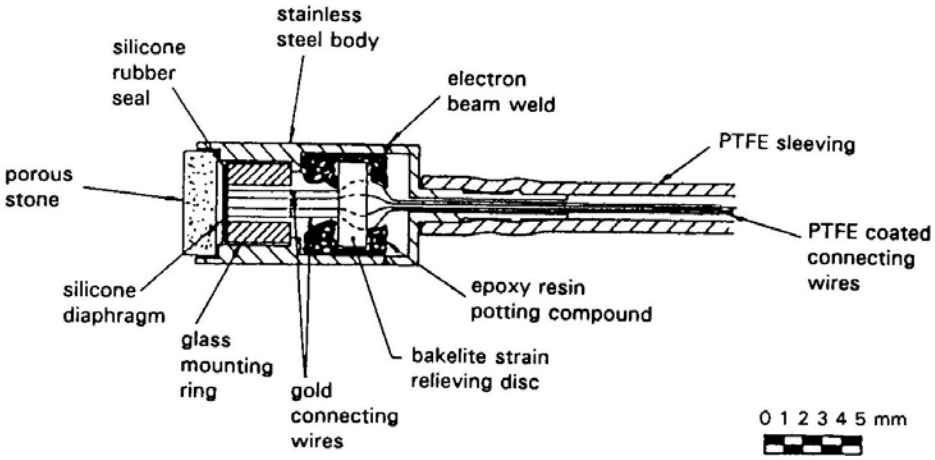

Figure 4.3: Schematic of a Druck PDCR81 PPT.

4.4.5 Accelerometers

Miniature piezo-electric accelerometers manufactured by DJ Birchall Ltd. were used to measure the accelerations in the model. The frequency response of these accelerometers has been shown to be flat (± 5%) from 20Hz to 2000Hz, Morris (1979). The typical calibration constant for these instruments varies from 6g/volt to 10g/volt. A typical transducer used in the centrifuge tests is shown in Figure 4.4. In the centrifuge tests described in this thesis, the fundamental earthquake shaking frequency is 50Hz and thus the accuracy in measuring the first five harmonics will be reasonably accurate. However, the low frequency response of the accelerometers is non-linear. Thus estimation of velocity and displacement by integrating the accelerometers signals are likely to be erroneous. This has been examined in some detail by Haigh (2002).

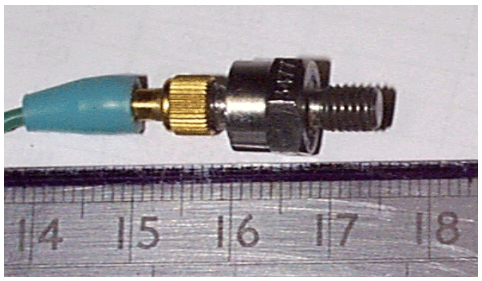

Figure 4.4: Accelerometer

4.4.6 Linearly Varying Differential Transformer (LVDT)

LVDT's were used to measure the displacements of the pile-cap in the vertical direction. They were powered by 10V AC supply. They had a maximum stroke length of ±22mm and were

calibrated against a micrometer through the junction box used in the centrifuge test. This is an electromagnetic device that produces an electrical voltage proportional to the displacement of a movable magnetic core. The calibration constant is typically 1.5 mm/volt to 3.5 mm /volt. Figure 4.5(a) shows a typical LVDT and Figure 4.5(b) shows the working principle. In the Figure 4.5(b) P denotes primary coil and S the secondary coil. When the magnetic core is displaced from null position, an electromagnetic imbalance occurs. This imbalance generates a differential AC output voltage across the secondary coils, which is linearly proportional to the direction and magnitude of the displacement

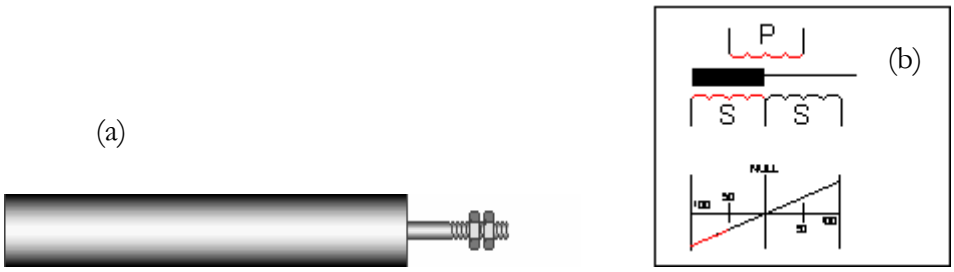

Figure 4.5; (a) L.V.D.T; (b): Working principle of LVDT.

4.4.7 Pressure transducer or Earth Pressure Cells

Miniature pressure transducers, Figure 4.6, manufactured by Entran were used to measure contact pressure on the front and back faces of model piles in one of the tests. This is a pressure sensitive device, which records the variation of pressure in the "pressure sensitive area", Figure 4.6(b), and subsequently changing the output potential (voltage). The pressure sensitive area has a flexible diaphragm, which deflects when loaded. These transducers have a 700kPa working range, as quoted, whereas the pressures measured were only of the order of 100kPa. Previous researches have shown that diaphragm stiffness of these transducers has a great effect on the pressure measured by them, Dewoolkar et al (1998). This is because as the diaphragm deflects, arching of the soil grains across the pressure sensitive diaphragm can result in lowering the pressure thereby giving erroneous results.

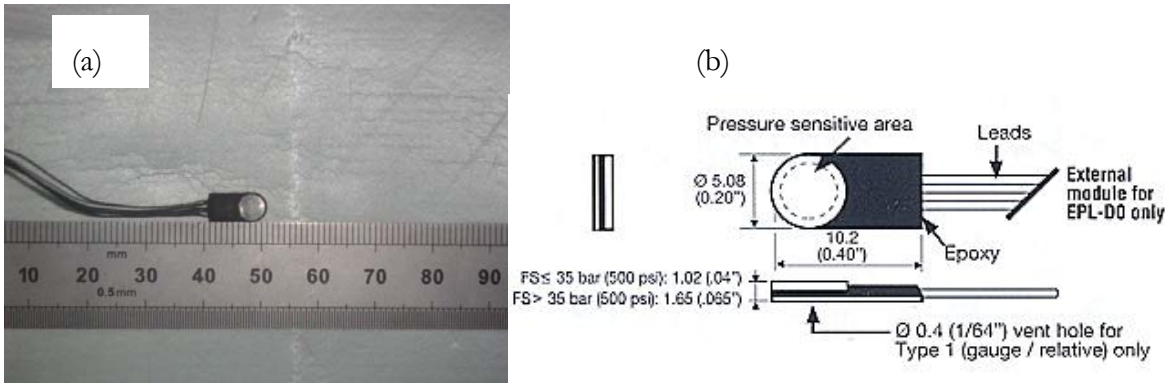

Figure 4.6 (a): Entran earth pressure cells; (b): Schematic details of the transducer

However, in dynamic testing, this may not be a problem as the inertial effects may destroy the arching action, Haigh (2002). The pressure transducers were attached to the model pile with double-sided tape as shown in Figure 4.7. Research is currently underway to understand whether the compressibility of the double-sided tape influences the readings of the stress cells.

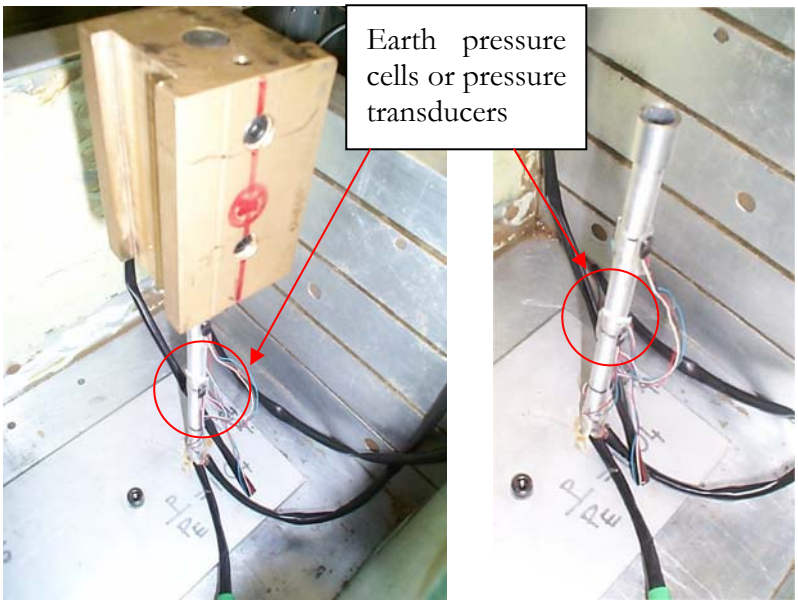

Figure 4.7: Pressure transducers attached in the piles

4.5 Centrifuge test program

Six centrifuge tests were carried out in level ground to study the effects of axial load on end-bearing piles as soil liquefies. Table 4.3 summarises the test program giving information on the soil profile, pile material and the pore fluid. It must be observed from Table 4.3 that the model pile material was changed from composite to dural alloy after the initial test SB-01. The development of the model piles is discussed in detail in section 4.6. As discussed earlier, buckling being the hypothesis to be verified, the choice of a suitable material for pile is very important.

Table-4.3: Test Program

Test ID	Soil profile	Pile material	Pore fluid	Remarks
SB-01	85mm fraction E sand underlying 20mm silt. (Relative density of sand was 47.4%).	Composite pile consisting of aluminium blades encased in a piece of relatively flexible high-density foam.	Water	The pile failed during the swing up, at 20-g, before firing the earthquake.
SB-02	150mm fraction E sand underlying 10mm silt. (Relative density of sand was 48.4%).	Aluminium alloy (Dural) tube. 3 piles were tested	Silicon oil 50 cSt	New pile material is used and it performed well. Behaviours of the pile under different loading regimes were studied.
SB-03	180mm fraction E sand. (Relative density of sand was 44.6%)	ditto	ditto	
SB-04	180mm fraction E sand (Relative density of sand was 43%)	ditto	ditto	
SB-05	No soil	Aluminium alloy (Dural) tube. 2 piles were tested	Air	
SB-06	180mm fraction E sand (Relative density of sand was 40 %)	Aluminium alloy (Dural) tube. 3 piles were tested	Silicon oil 50 cSt.	

4.5.1 Sand used in the tests

Fraction E silica sand prepared to relative density of around 50% (see Table 4.3) was used in each model. Table 4.4 shows the properties of the sand. This sand was used by earlier researchers to study soil liquefaction problems, for example Haigh (2002), Brennan (2003). This soil also falls within the boundaries for most liquefiable soil in Tsuchida's grain size distribution curve as discussed in section 2.2.4

Table-4.4: The properties of the sand after Tan (1990).

D_{10} grain size	0.095 mm
D_{50} grain size	0.14 mm
D_{60} grain size	0.15 mm
Specific Gravity G_s	2.65
Minimum Void ratio e_{min}	0.613
Maximum Void ratio e_{max}	1.014
Permeability to water (e = 0.72)	0.98 E -04 m/s
Angle of shearing resistance at critical state ϕ_{crit}	32^0

4.5.2 Earthquake input motions

Earthquakes are, by nature, random and unpredictable. The time of an earthquake at any place can only be predicted in the order of geological years, but areas prone to earthquake can be mapped based on fault geometry. Each earthquake is also unique in magnitude, duration and frequency content. It has been widely accepted that there is not much similarity between two consecutive earthquakes even at the same location. Figure 4.8(a) shows the input motion of the 2001 Bhuj earthquake (India), as recorded in the Passport Building at Ahmedabad. The earthquake had a duration of 32 sec and the peak acceleration measured was 0.1g. From the accelerometer readings it must be noted that the motion had multiple frequencies of different magnitudes. Two approaches emerge in modelling earthquake input motion in centrifuges, as follows:

In one approach, an earthquake similar to a real earthquake having multiple frequencies, for example El Centro motion, can be modelled. This requires a very complicated and expensive actuator. In the other approach, a motion having predominantly a single frequency may be modelled. This requires a relatively simple and inexpensive actuator.

The "Cambridge philosophy" has been in favour of providing a single frequency input motion to models. Ghosh and Madabhushi (2003) compared the two approaches and concluded that it is much simpler to analyse the behaviour of dynamic events under single frequency earthquake input motions. This is because a particular behaviour, for example frequency of cycling of pore pressure, may be examined in relation to the single input frequency. On the other hand, multiple

frequencies could complicate this behaviour and no definite conclusion could be derived. It may also be argued that in order to reproduce the behaviour of real structures under real earthquakes it may be necessary to model the real input motion.

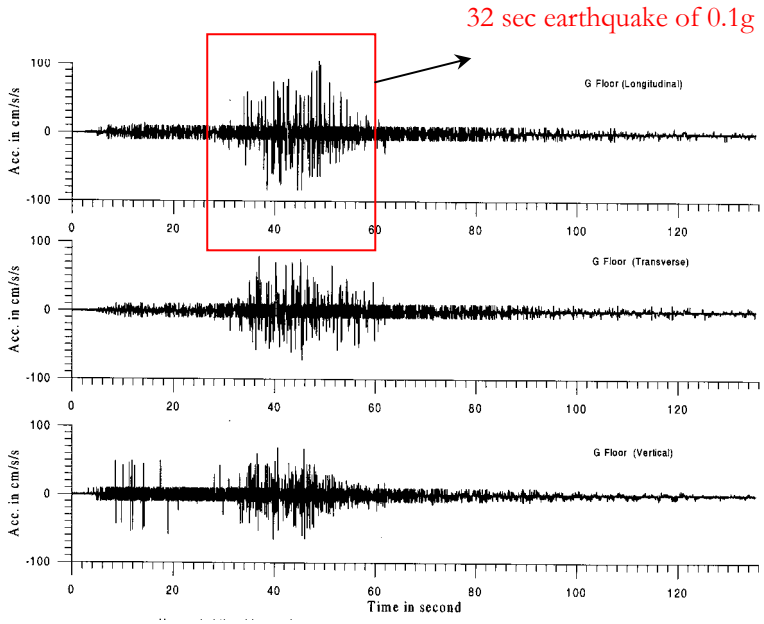

Figure 4.8(a): Earthquake motion of Bhuj earthquake as recorded in a building, Roorkee (2001).

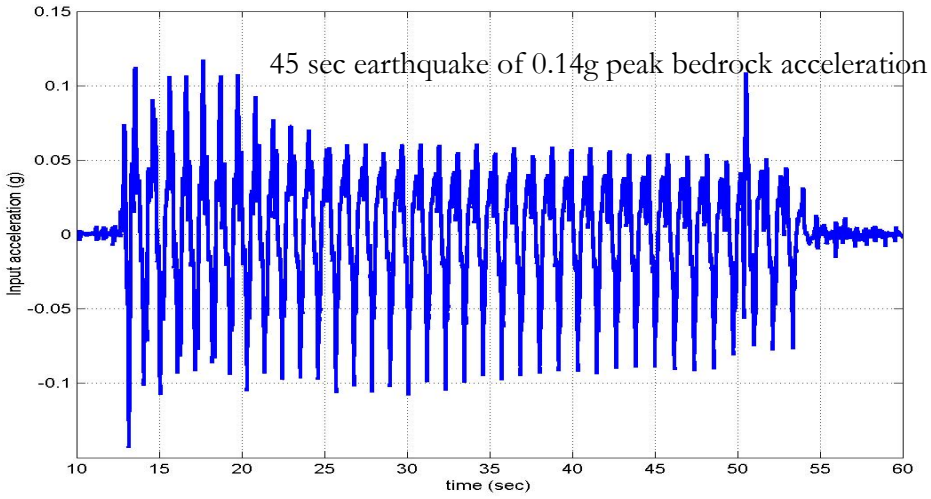

Figure 4.8(b): Typical input motion used in the centrifuge tests.

However, in the tests described in this thesis, the earthquake input motion is required only to liquefy the soil and the controversy over the type of motion can be safely ignored. A typical earthquake input motion in the centrifuge tests is shown in Figure 4.8(b) in prototype scale. The motion had 1 Hz frequency, 45 sec duration 0.14g peak "bedrock" acceleration. The motion is predominantly one-dimensional. The cross acceleration was measured to be 0.5% of the lateral acceleration.

4.6 Development of model pile

This investigation was performed as a part of ongoing research undertaken at Cambridge to gain an insight into the failure mechanism of piled foundations in areas of seismic liquefaction. Haigh (2002) in Cambridge used a composite pile constructed from a pair of thin flat aluminium blades encased in a piece of relatively flexible high-density foam with adhesives to study the lateral spreading effects on piled foundations in absence of axial loads. The advantage of using this type of pile is to have larger strain for a low load thus having a very good measurable response. The section of the pile is shown in Figure 4.9 and the pile is shown in Figure 4.10.

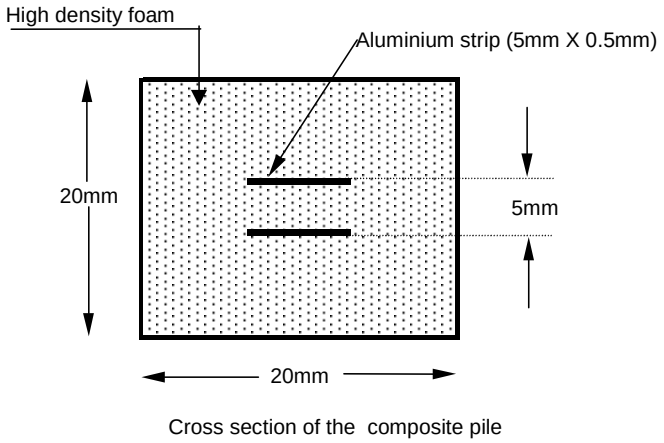

Figure 4.9: Pile section used in test SB-01

This pile was used in the test SB-01 to study the axial load effects on the pile in a level ground. The idea of using this composite pile was to compare with the results of lateral spreading effects on pile carried out by Haigh (2002). Superposition of the results of the two primary load cases could suggest the overall response of pile foundation in sloping ground.

Figure 4.10: Composite pile used in test SB-01.

As mentioned in Table 4.3, this composite pile was used in test SB-01 but the pile failed before the earthquake could be fired. It was realised that this composite material is not suitable for this research because it was too weak in buckling. In the subsequent tests, an aluminium tubular pile was used and it performed very well. This section of the chapter will discuss the difficulties of characterising the composite pile and how the current model pile was designed.

4.6.1 Characterisation of composite pile

Tests were carried out to find the suitability of this type of composite pile for axial response. Two composite piles as listed in Table 4.5, and a pure foam pile were tested in the Instron Machine to find the failure load in buckling. The jaws of the Instron Machine simulated approximately fixed boundary conditions at both ends of the sample. The stress strain plot for the pure foam of size 20mm × 20mm is shown in Figure 4.11. The Young's Modulus estimated for this foam material is 6.2 MPa. The sample failed at 58 N (i.e. at 0.14 MPa stress).

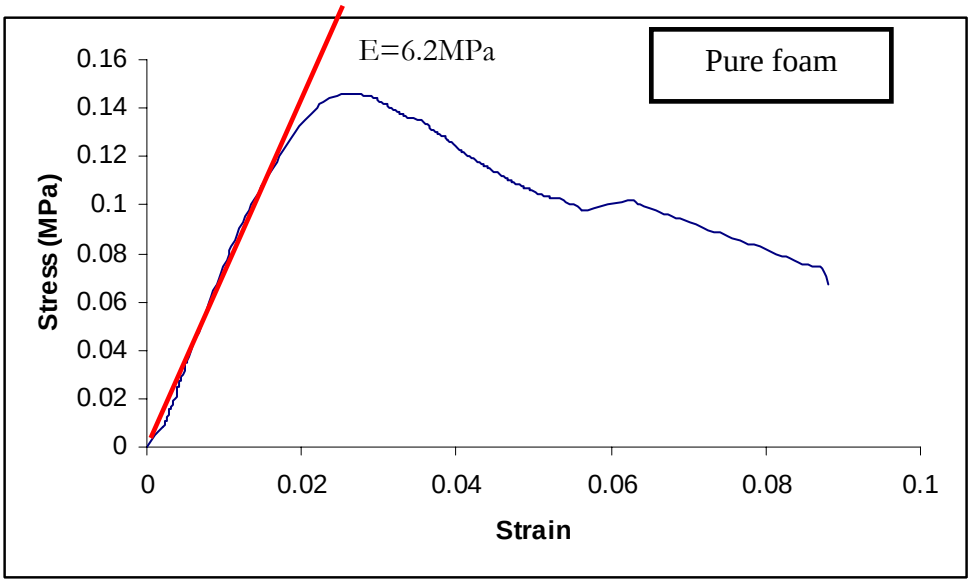

Figure 4.11: Stress-strain plot of high-density foam cube of size 20mm × 20mm.

Two composite piles of different lengths and different overall dimensions (but the spacing and size of the aluminium blades were same) were tested. Table 4.5 summarises the cross section, length and failure load of the composite piles.

Table 4.5: Composite pile test program and failure load.

Pile ID	Length	Cross-sectional area	Failure load
P-1 (Reinforced foam as shown in Figure 4.9)	123 mm	20mm × 20 mm	318 N
P-2 (Reinforced foam as shown in Figure 4.9)	80mm	20mm × 16 mm	192 N

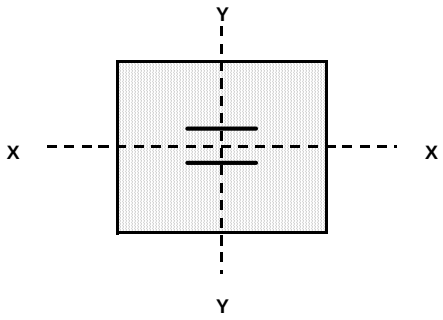

Figure 4.12: Schematic diagram of composite pile showing the axes.

Table 4.6 shows the predicted capacity of the composite section. The Young's Modulus of Aluminium alloy is 70GPa compared to 6.2MPa of foam. In the calculation, it is assumed that foam between the two aluminium strips acts a weak web of an I-section and has no contribution in the stiffness of the composite section. The critical load is estimated assuming both ends to be pinned.

Table 4.6: Table showing the predicted properties of the composite section.

Pile ID	I_{XX} (mm^4)	I_{YY} (mm^4)	$P_{cr, xx}$	$P_{cr, yy}$	Actual failure load
P-1	25.4	10.4	1160 N	476 N	318 N
P-2	25.4	10.4	2742 N	1125 N	192 N

It was observed during the test that both the piles failed about X-X axis (see Figure 4.12). If the section acted as a composite it would have failed about weaker axis i.e. Y-Y as shown in Figure 4.12.

Figures 4.13 and 4.14 show the stress-strain plot for the above two piles. The stress-strain plot for the two piles shows a distinct feature. In the plot for pile P-1 the Young's Modulus of the composite is 123 MPa whereas for pile P-2 there are two gradients. The initial gradient is 11.8 MPa and the steep gradient is 100 MPa. Due to unevenness of the cross-section, the applied load may be taken initially either by aluminium or foam or combined. This might explain the two different gradients in the stress-strain plot for pile P-2.

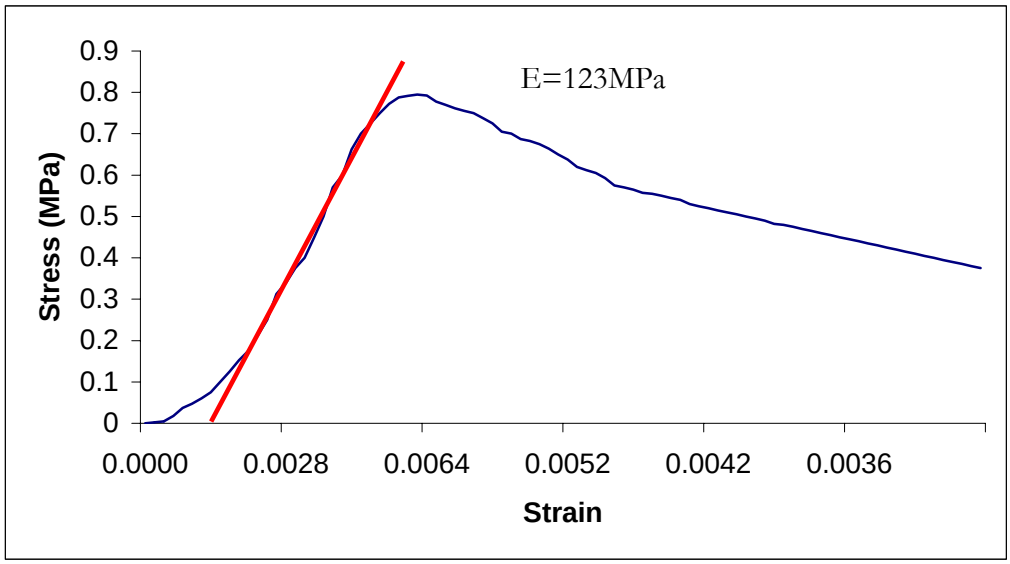

Figure 4.13: Stress-strain plot of aluminium reinforced high-density foam pile (marked P-1) 123 mm long. The section is shown in Figure 4.9.

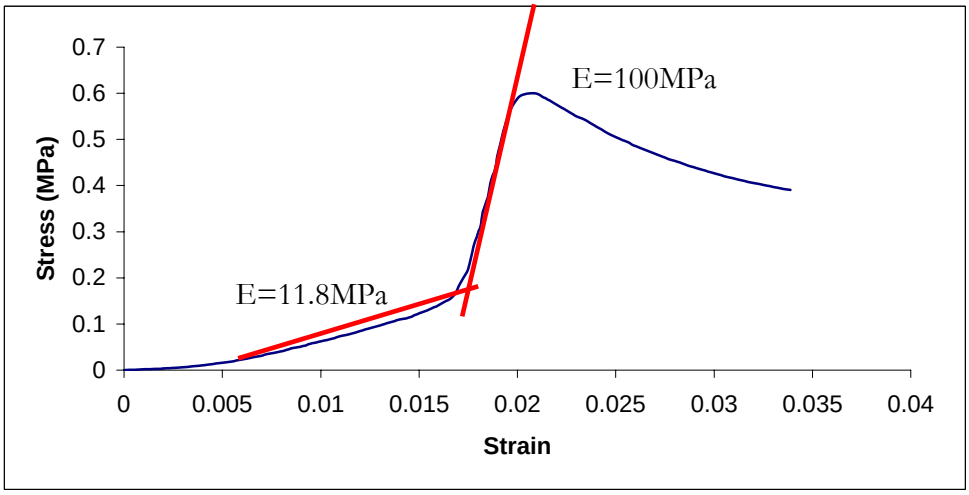

Figure 4.14: Stress-strain plot of aluminium reinforced high-density foam pile (marked P-2) 80 mm long. The section is similar to Figure 4.9 but the size of pile is 20mm × 16mm.

Several theoretical back-calculations were tried to predict the load carrying capacity but a suitable theory was not obtained. This pile was used in test SB-01 but the pile failed before the firing of earthquake. Many uncertainties are involved in determining the strength of this type of pile, such as adhesive bond strength, levelled edge surface. For obvious reasons such material is not feasible for verifying buckling mechanism.

This led to a reconsideration of suitable pile material.

4.6.2 Choice of model pile

The aim of this research is to understand the effect of axial load on a pile as the surrounding soil liquefies. Axial load will be applied through a block of brass attached to the head of the pile (Figure 4.7) and with the increase in centrifuge acceleration the mass will progressively apply more load in the pile.

The following items are likely to influence the behaviour of a pile of this kind:

1. Effects of imposed axial load
2. Soil-pile inertial interaction i.e. inertial effects of the mass at the top.
3. Soil-pile kinematic interaction i.e. soil flow, if any, past the pile.
4. Pile radiation damping.

In the present research, the main aim is the response of an axially loaded end bearing pile due to soil stiffness degradation associated with liquefaction. Soil pile interface friction along the shaft (shaft resistance) constitutes a secondary factor for the axial response of an end bearing pile during earthquake liquefaction. This is because of the fact that the pile will lose a significant amount of shaft resistance when the surrounding soil liquefies. It was realised that there are many factors that may dictate the design of a model pile. They can be grouped into three categories as discussed below.

1. **Structural properties**: Buckling is very sensitive to imperfections, such as irregularity in shape and size, initial curvature and variation in material in-homogeneity. The structural properties identified for model pile design are as follows:
    - Euler's buckling load or critical load, P_{cr}
    - Diameter to thickness ratio (d/t) for local buckling of pipe piles.
    - Effective length (L_{eff}) and slenderness ratio (L_{eff}/r_{min})
    - Flexural stiffness (EI) and axial stiffness (EA).
    - Yield behaviour and moment – curvature relationship
    - Natural period of the system to avoid resonance.
2. **Modelling constraints**: In centrifuge testing, a minimum diameter of the pile has to be maintained to avoid particle size effects. Bolton et al (1999) examined different CPT probes and concluded that the cone diameter should be at least twenty times greater than the mean particle diameter D_{50}. Thus the minimum pile diameter should be 2.8mm for fraction E sand.
3. **Practical constraints**: There is a restriction in the length of the pile due to limited size of the ESB box. In addition, the mass to be placed at the top should contribute minimal inertial effects to the pile.

Three materials were investigated to ascertain their suitability as a model pile material.

Table 4.7: Properties of potential pile material

Materials	**Elastic Modulus**	**Yield stress**
Copper	130GPa	210MPa
Steel	210GPa	400MPa
Aluminium	70GPa	250MPa

Among the above materials, for a particular cross-section and length, the critical load for an aluminium pile is the least and hence a smaller brass block will be required to simulate P_{cr} at 50-g. A spreadsheet was prepared to fit all the modelling parameters, viz. the length of the pile, Euler's buckling load, slenderness ratio and the mass required to be placed at the top. This is shown in Table 4.8.

Table 4.8: Spreadsheet used to choose the suitable pile section. The section of the pile shown in shaded row was used for the test SB-02

Data

E = 70 GPa, Length = 160mm

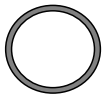

Section of the pile

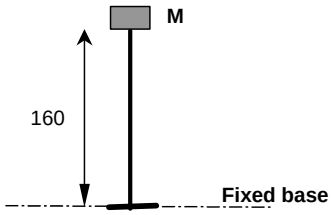

Outside dia (mm) d_0	Inside dia(mm) d_i	wall thickness (mm) t	Second moment of area (mm^4)	EI ($N\ mm^2$)	Critical buckling load assuming cantilever (kg)	radius of gyration , r_{min} mm	Model mass at 50 g in Kg (M)	l/rmin	(d_i/t) internal dia./thickness
19.05	17.25	0.9	2118.4	1.48E+08	1458.3	6.4	29.2	50	19.2
17.7	17.25	0.225	471.6	3.30E+07	324.6	6.2	6.5	52	76.7
17.5	17.25	0.125	257.5	1.80E+07	177.3	6.1	3.5	52	138.0
12	11	0.5	299.2	2.09E+07	206.0	4.1	4.1	79	22.0
11.5	11	0.25	139.9	9.79E+06	96.3	4.0	1.9	80	44.0
9.5	8.5	0.5	143.6	1.01E+07	98.8	3.2	2.0	100	17.0
9.4	8.5	0.45	127.0	8890703	87.4	3.2	1.7	101	18.9
9.3	8.5	0.4	111.0	7.77E+06	76.4	3.1	1.5	102	21.3
9.2	8.5	0.35	95.4	6.68E+06	65.7	3.1	1.3	102	24.3
9.1	8.5	0.3	80.4	5.63E+06	55.3	3.1	1.1	103	28.3
9	8.5	0.25	65.8	4.61E+06	45.3	3.1	0.9	103	34.0

A sample calculation for the shaded row in the Table 4.8 is shown below.

- The second moment of area (I) = $\frac{\pi}{64}\left(d_0^4 - d_i^4\right) = 95.4\ mm^4$
- Flexural stiffness (EI) = 95.5 $mm^4 \times 70$ GPa = 6.68×10^6 N.mm^2

- Effective length = 2 × 160 mm = 320 mm
- Critical load is calculated from Euler's formula and is 65.7 kg.
- The radius of gyration of this tubular section is calculated to be 3.1mm.
- The load to be applied at the top of the pile at 1-g to get 65.7 kg at 50-g is 1.3 kg.

An Aluminium alloy pile having the properties shown in Table 4.9 is used in the centrifuge tests.

Table-4.9: Properties of model pile used in the tests

Material	Aluminum alloy (Dural)
E (Young's Modulus)	70GPa
Outside diameter	9.2mm in SB-02 9.3mm in SB-03, SB-04, SB-05 & SB-06
Inside diameter	8.5mm
Length	160mm for SB-02 180mm for SB-03, SB-04, SB-05 & SB-06
Yield Stress	250MPa
Diameter/thickness ratio	25 for SB-02 22.25 for SB-03, SB-04, SB-05 & SB-06

4.7 Structural testing of model pile

The model piles used in the centrifuge tests were machined from a thick walled tube (2mm) to the required thickness (0.4mm). It was realised that, as buckling is sensitive to imperfections, structural testing of some of the piles will provide greater confidence on the quality of the piles. Buckling load tests and a plastic moment capacity test were carried out to compare with the theoretical estimates.

4.7.1 Buckling test of the model piles treated as struts

Buckling tests of two model piles were carried out to compare the theoretical critical load with the experimental value. The piles being thin walled raise a question of interaction between local buckling and Euler's buckling of the entire strut. The experiments also present an opportunity to investigate the post buckling behaviour of the pile, i.e. the behaviour after the peak load has been exceeded. This section will discuss the results of the buckling tests carried out on the model piles. Table 4.10 summarises the results of the buckling tests on the two model piles.

Table 4.10: Buckling test on the model piles

Buckling test ID	**Pile details**	**End conditions in an Instron machine**	**Theoretical estimate of the buckling load**	**Experimental buckling load**	**Remarks**
BT-1	200mm long	The pile was held in position by the top and bottom platens of the Instron machine (see Figure 4.15).	1.917 kN (Assuming both ends pinned)	2.557 kN	From the mode shape (Figure 4.17) it is clear that the bottom end of the pile had partial fixity.
BT-2	200mm long	Two circular plates (10mm thick) were glued at the end of the piles (see Figure 4.18.)	2.36kN for 180mm long (assumed both ends pinned)	2.01 kN	The end condition were approximately pinned-pinned, (Figure 4.18)

(a) 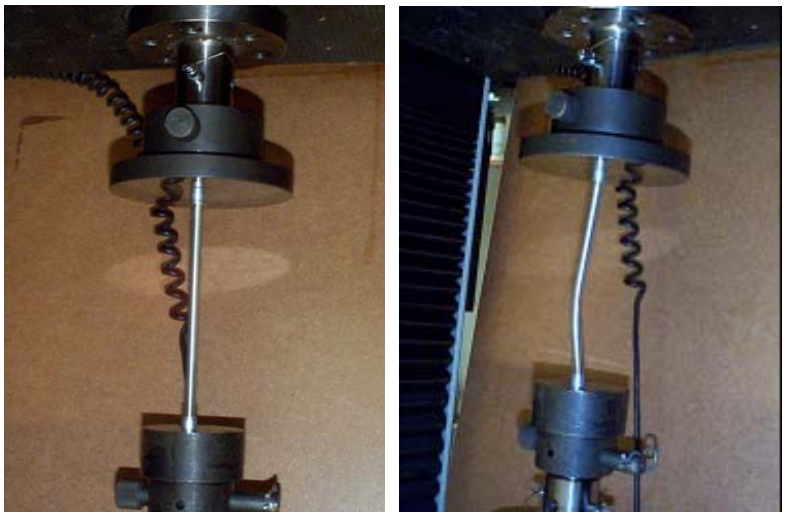 (b)

Figure 4.15: Buckling test BT-1; (a): Before the test; (b): After the test.

Figure 4.16 shows the load deformation characteristics of the pile in test BT-1. The experimental critical load is 33% higher than the theoretical critical load assuming the end conditions to be pinned-pinned. It must be noted from the mode shape (Figure 4.17) that the platens of the Instron machine offered some fixity to the pile.

In test BT-2, a similar pile was tested. This pile had two circular plates (10mm thick) co-centrically glued to the pile at both ends as shown in Figure 4.18 (a). The theoretical estimated

buckling load is any value between 1.917kN (200mm length) and 2.36kN (180mm). The pile actually buckled at 2.01kN. From the buckled shape, Figure 4.18 (b), it may be concluded that the end conditions were approximately pinned at both ends. Figure 4.19 shows the load deformation characteristics of this pile.

The imperfections associated with the buckling test of columns can be divided according to their effects in three groups, after Salmon (1921). They are

1. Eccentricity of loading
2. Initial curvature
3. Reduction in strength of material

In reality, it is very difficult to avoid all imperfections and this was also not the primary aim of this research investigation. However, it may be concluded that the model piles did not buckle prematurely due to local buckling.

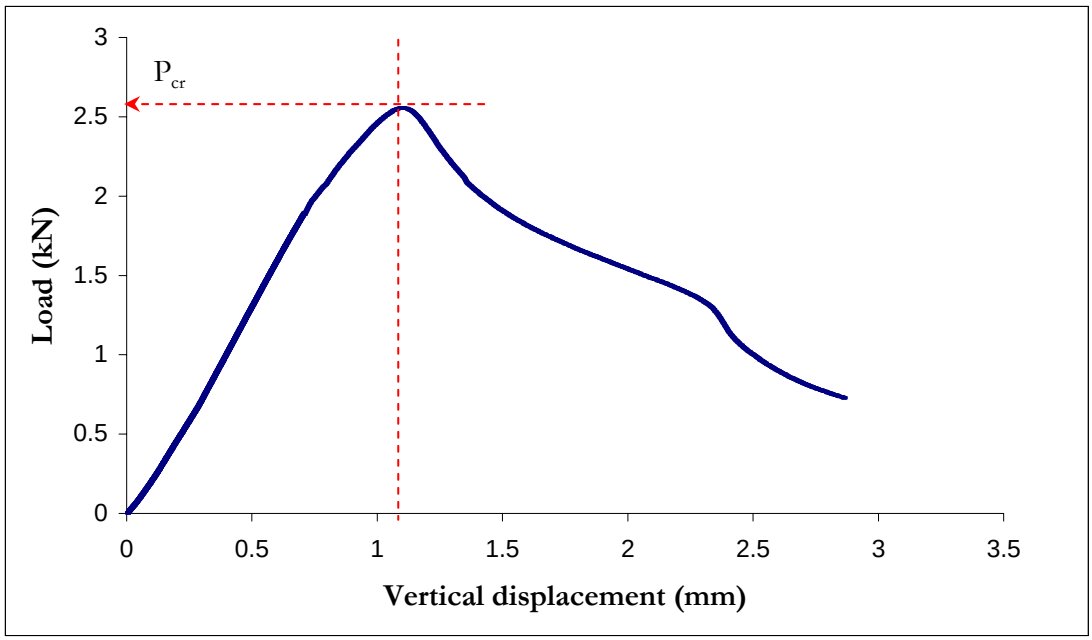

Figure 4.16: Load-displacement plot for the buckling pile in test BT-1

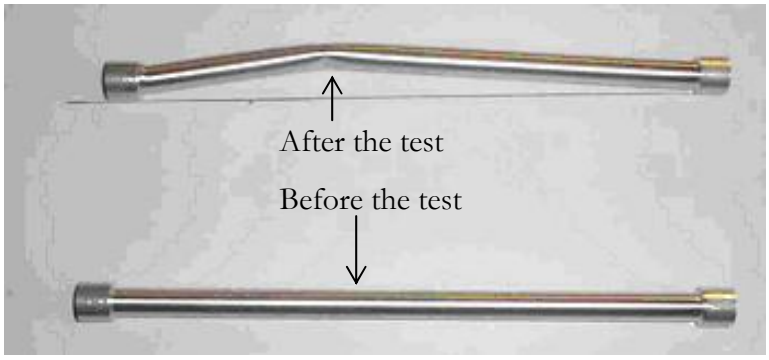

Figure 4.17: Buckling mode shape in test BT-1

(a)

(b)

Figure 4.18: Buckling test BT-2; (a): Before the test; (b): After the test.

In centrifuge tests, end conditions of the pile may not be a potential problem. The piles in the centrifuge tests were the simplest form of column i.e. cantilever and hence there is only one boundary condition to be simulated. It is also relatively easy to simulate a fixed end condition.

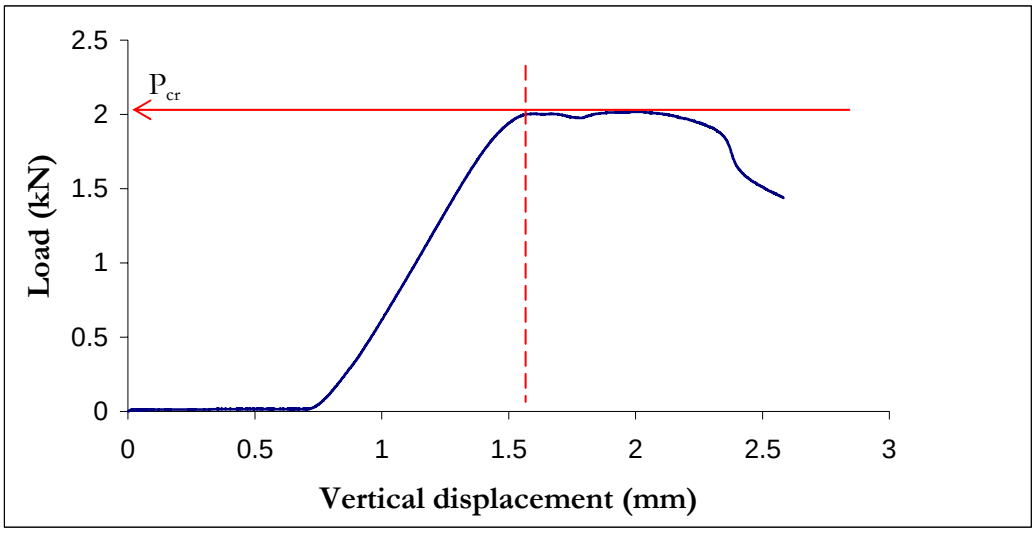

Figure 4.19: Load-displacement plot for the buckling pile in test BT-2

4.7.2 Plastic moment capacity of model pile

A test was conducted to measure the plastic moment capacity of the pile section. The experimental set up of a 4-point bending test is shown in Figure 4.20. The load was applied in two positions and the central deflection was measured. The central portion of the beam has a constant moment and no shear force, which is often termed as pure bending by structural engineers. The end conditions were purely simply supported. The test is load-controlled and the load is increased gradually until the section forms a plastic hinge. From the central deflection the curvature was estimated. Figure 4.21 shows the plot of load versus central deflection. Based on the test data the measured plastic moment capacity of the section is 8175Nmm.

The theoretical estimate $= \left(\frac{9.3^3}{6} - \frac{8.5^3}{6} \right).250 Nmm = 7925 Nmm$

The moment curvature relationship for the pile is shown in Figure 4.22 and the curve is of bi-linear nature. In the figure A represents the first yield moment of the section i.e. the moment at which the section of the pile first attains yield in the extreme fibre. Point B in the same figure signifies the fully plastic moment which corresponds to the spread of the plastic zone across the entire cross section. It must be noted that after this point large changes in curvature occurred with no change in bending moment.

As can be seen from Figure 4.21, the model pile can deform elastically 4mm i.e. (Length/40) before reaching the first yield. It will be shown in section 4.8 that ductile concrete columns have a similar type of yield behaviour.

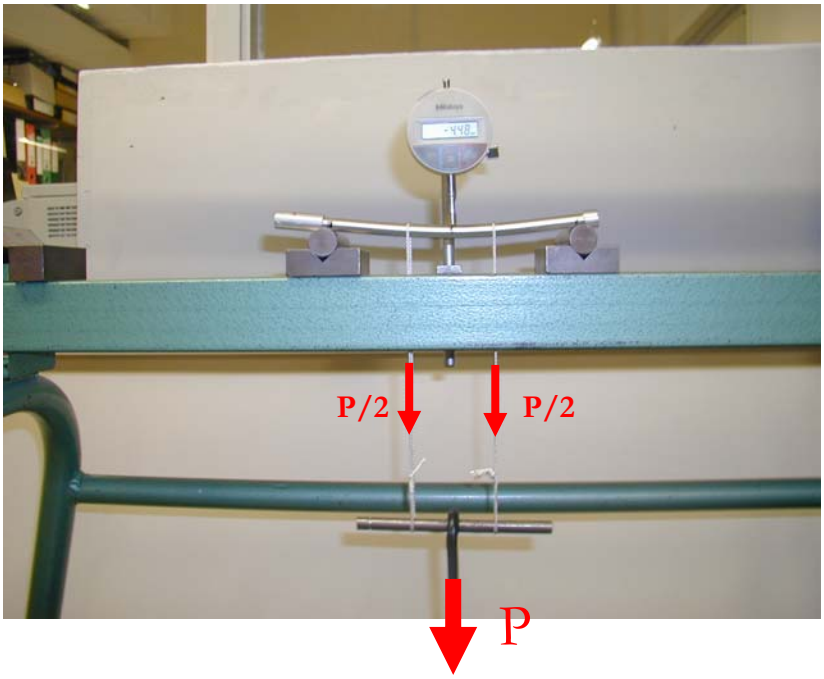

Figure 4.20: Experimental set up for measuring plastic moment capacity.

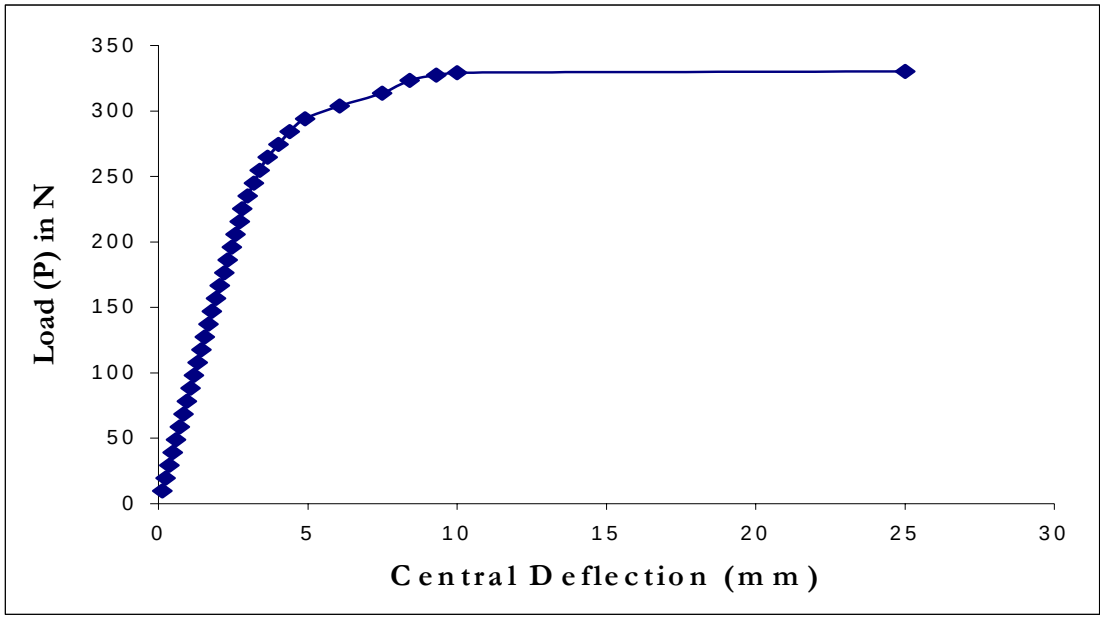

Figure 4.21: Load (P) – deflection curve in the M_p test (Figure 4.20) of the pile.

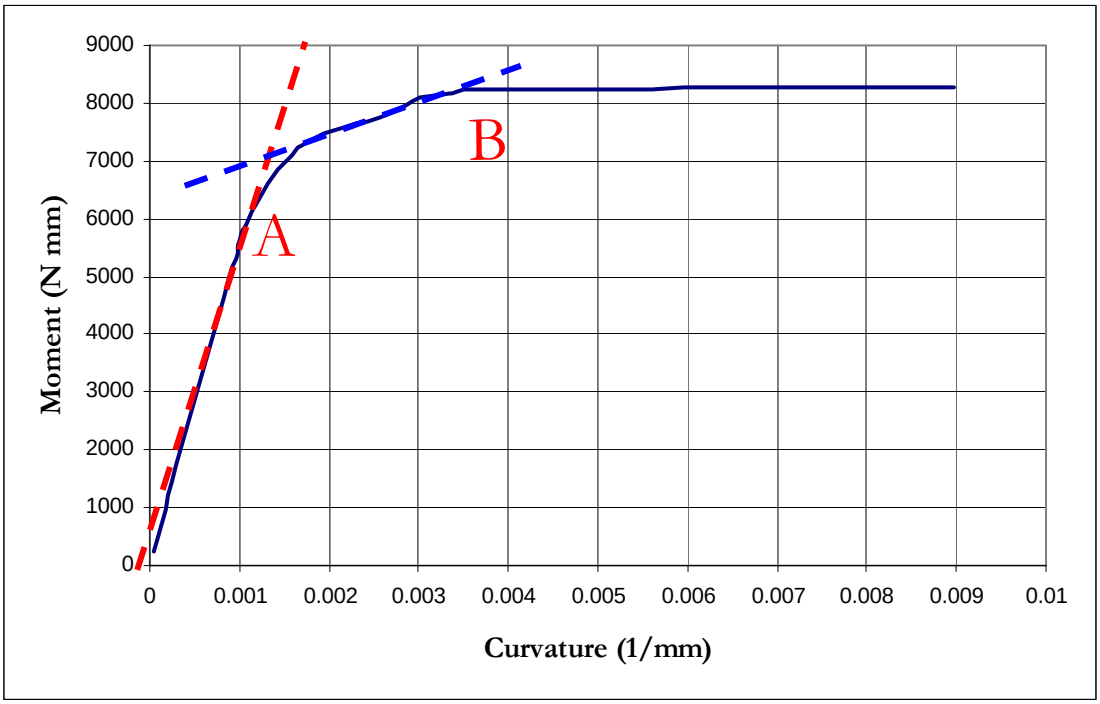

Figure 4.22: Moment–curvature relationship observed in a model pile in the M_P test (Figure 4.20).

4.8 Comparison of a prototype pile with an equivalent real pile

This section of the chapter compares the prototype pile with an equivalent real pile. Normally, piles are made up of reinforced concrete or steel. Using the principle of transformation of section, the prototype dural alloy pile is transformed into an equivalent hypothetical concrete and steel pile section. Table 4.11 shows the properties of model and prototype pile linked through the scaling laws discussed in Table 4.1.

Table 4.11: Properties of model pile and its prototype at 50-g

Properties	Model	Prototype section (50-g)
Material	Aluminium Alloy (Dural)	Aluminum Alloy (Dural)
E (Young's Modulus)	70 GPa	70 GPa
Outside diameter	9.3 mm	465 mm
Inside diameter	8.5 mm	425 mm
r_{min} of the section	3.1 mm	155
Yield Stress	250 MPa	250 MPa
Plastic moment capacity (M_p)	8175 Nmm	8175 x 50^3 = 1021.8 kNm
EI of the section	7.77 × 10^6 Nmm^2	7.77 × 10^6 x 50^4 = 48.6 x10^3 kNm^2

4.8.1 Transforming the prototype dural alloy section into an equivalent hypothetical concrete section

Modular ratio = $\frac{E_{dural}}{E_{concrete}} = \frac{70GPa}{22.5GPa} = 3.1$

Thickness of an equivalent concrete pile section = 20 × 3.1 = 62mm, Figure 4.23.

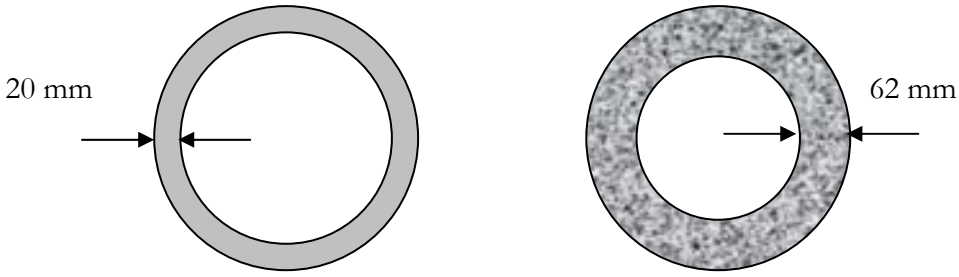

Figure 4.23: Transformation of dural alloy pile section to an equivalent concrete pile section keeping the same mean diameter (445 mm).

Properties of a hypothetical concrete pile section

Grade of concrete = M25 i.e. f_{ck} = 25 MPa

Outside Diameter = 507mm

Inside Diameter = 383mm

E of concrete = 22.5GPa

Allowable bending strength in compression = 0.446 f_{ck}=11.2MPa.

$M_p = (\frac{0.507^3}{6} - \frac{0.383^3}{6}) \times 11.2MPa$ = 138 kNm

EI = 49.2 x 10^3 kNm^2.

r_{min} = 159mm

The model pile used in the centrifuge test is 7 times stronger than an equivalent concrete pile of same stiffness in terms of plastic moment (M_p). Figure 4.24 shows the moment-curvature relation for circular concrete columns, which is similar in nature to the model pile in absence of soil (Figure 4.22).

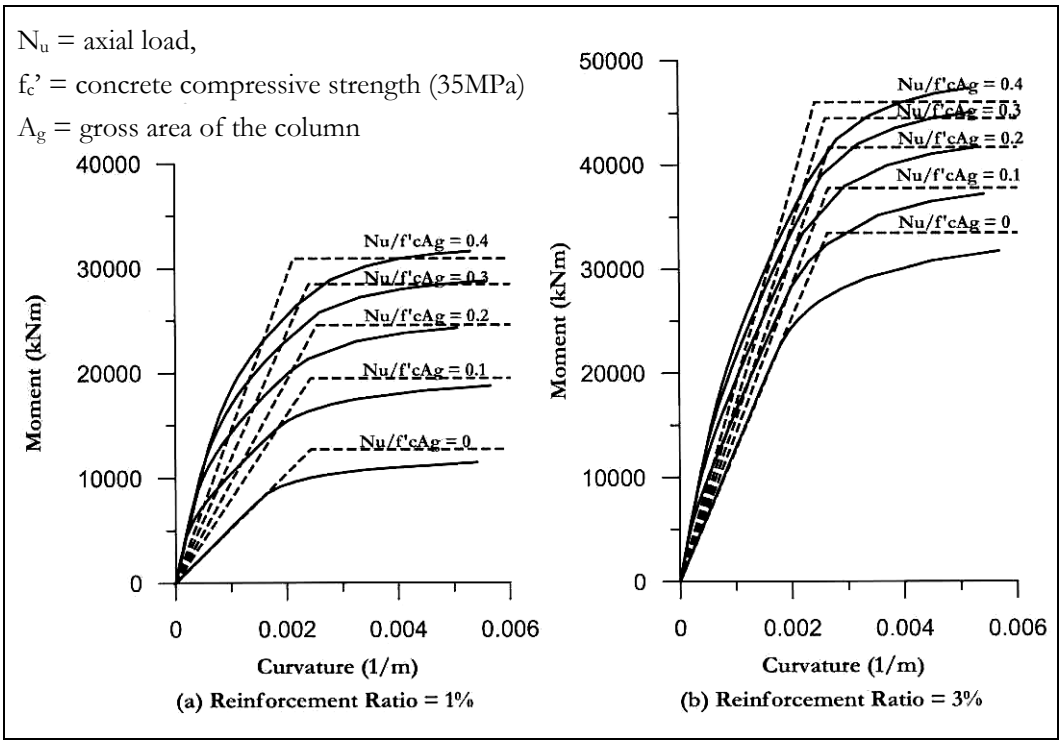

Figure 4.24: Moment-curvature curves for circular columns for different axial load ratio, Priestley (2003). f_c' is same as f_{ck}.

4.8.2 Transforming the prototype Dural alloy section into an equivalent hypothetical steel tubular section:

Modular ratio = $\frac{E_{dural}}{E_{steel}} = \frac{70GPa}{210GPa} = 0.33$

Thickness of an equivalent concrete pile section = 20 × 0.33 = 6.6mm

Properties of a hypothetical steel pile section

Thickness = 6.6mm

OD = 445 + 6.6 mm = 451.6mm

ID = 445-6.6mm = 438.4mm

$M_P = (\frac{0.452^3}{6} - \frac{0.438^3}{6}) \times 500MPa$ = 693 kNm

r_{min} = 157.3mm

EI = 48 x 10^3 kNm^2

Thus the model pile used in the centrifuge test is 1.5 times stronger than an equivalent steel pile in terms of plastic moment (M_p).

4.9 Model preparation and test procedure

The model is prepared at 1-g in the model preparation room. The piles are rigidly fixed to a frame and the frame is attached to the base of the ESB box, Figure 4.25. The pile head masses are taken out during sand pouring to avoid obstruction. The pile installation effects are not modelled. Sand is poured by air-pluviation into the ESB box using the overhead hopper. Uniformity in flow of sand in the hopper is maintained by controlling the height of fall of sand and the aperture of the hopper. This allows the sand in the model to be approximately of uniform density. Sand is poured in layers depending on the number of layers of instruments used.

Accelerometers and PPT's are placed as per designed layout. Accelerometers are placed horizontally along the direction of shaking and PPT's are placed perpendicular to the shaking. After the completion of sand pouring in the model with the burying of instruments, the ESB box is made airtight using the lid. The package is then connected to a silicone oil tank through the orifices at the bottom of the box and also to a vacuum pump through a valve at the top of the lid. Any entrapped air in the model is removed by the vacuum pump before allowing the model to suck silicone oil. The pump generates a suction of 70kPa to 80kPa within the model and this results in the oil entering the model. The rate of oil flow is maintained very low, in the order of 0.5 kg per hour, to avoid liquefaction phenomenon. After the saturation is complete the pile head masses and the LVDT's are fixed in place (see Figure 4.26).

TEST PROCEDURE

The package is placed in the centrifuge and spun in steps of 10-g, 20-g, 40-g and 50-g. The pore pressure and LVDT data are logged to have checks and balances in the instrument readings. At 50-g the earthquake is fired using the SAM actuator. The frequency of the earthquake was 50Hz and the earthquake duration was 0.5 sec to 0.9 sec. This would replicate 1 Hz prototype earthquake of 25 sec to 45 sec duration. CDAQS was used for data acquisition.

TEST SB-01

As mentioned earlier, this was an initial test and the pile failed before the firing of an earthquake. The test produced data equivalent to a real earthquake. However the tests results do not have relevance with the aims and scope of the work. The results of this test will not be discussed any further.

TEST SB-02

This test simulated axially loaded end bearing piles passing through liquefiable sand. The model consisted of three piles carrying different axial loads and was conducted at 50-g. The layout and instrumentation of the model is described in chapter 6. The soil profile and pore fluid used in the test are mentioned in Table 4.3. The pile was fixed at the base and also to the brass weights as

shown in Figure 4.25. The bulk density of the fully saturated soil was 18.68kN/m^3 and the submerged unit weight is 8.8kN/m^3. The model was placed on the SAM actuator, as shown in Figure 4.26 and spun in the centrifuge to 50 g in steps. In this acceleration field, the model represented a prototype of 7.5 m thick loose saturated sand underlying 0.5 m silt (rock flour) having infinite lateral extent. The intention of putting the silt layer was to hold the excess pore pressure for longer duration. One-dimensional shaking was imparted along the model base using SAM actuator for 0.5 seconds with a frequency of 50 Hz. Thus in the prototype (according to scaling laws in Table 4.1) the above shaking simulated a 25 second earthquake of 1 Hz frequency. Accelerations pore pressures and displacements were recorded using installed transducers.

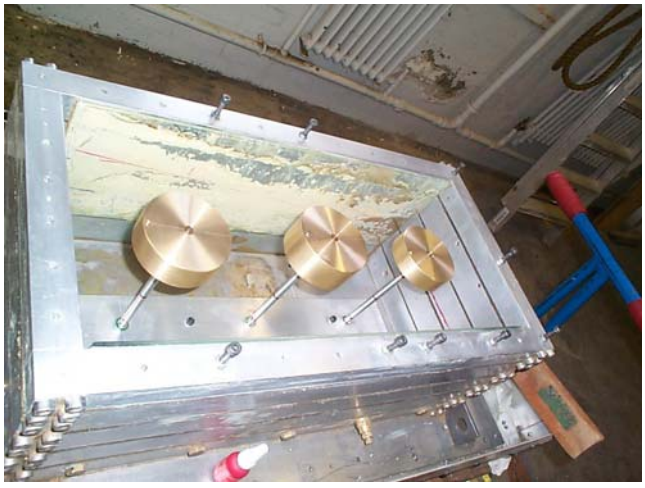

Figure 4.25: The piles and the pile head masses. The piles are fixed at the base. Pile head masses are taken out during sand pouring.

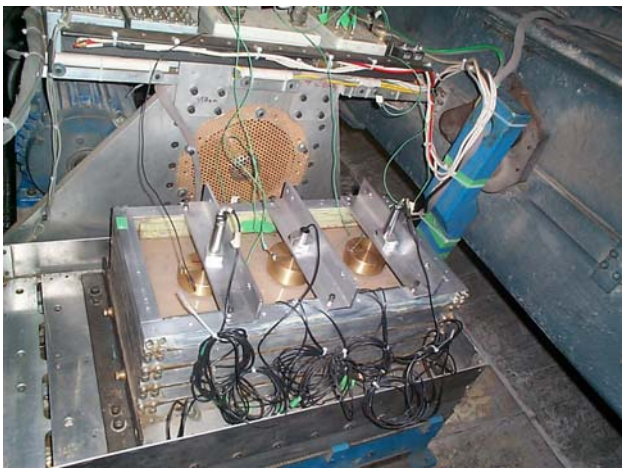

Figure 4.26: The package resting in the SAM ready to be centrifuged.

Two of the piles failed during swing up and one of them failed as the earthquake was fired. Following this, the load effects that control pile failure during centrifuge tests had to be reconsidered.

4.10 Factors controlling failure of a pile in a centrifuge test

Following test SB-02, it was realised that there are three load effects, which control the pile failure mechanism in the centrifuge in the absence of lateral spreading:

1. 1-g effect of Earth's gravity on the pile head mass [imperfection lateral load].
2. N-g effect of centrifuging the pile head mass [axial load]
3. Inertia force induced during earthquake shaking.

A schematic diagram showing the basic principle of the experiments is shown in Figure 4.27. This figure also shows the load effects. A block of brass fixed at the pile head as shown in Figure 4.28 is used to simulate the axial load in the pile in all the tests. With the increase in centrifugal acceleration to N-g, the brass weight imposes increasing axial force in the pile as shown in Figure 4.27. One problem of using a brass weight is the action of Earth's gravity by which the resultant load acting on a radial pile is not purely axial. At lower g-levels especially, the soil may not gain enough confining pressure to prevent the pile deflecting under disproportionately large lateral forces, and the experiment may therefore begin with an initial imperfection.

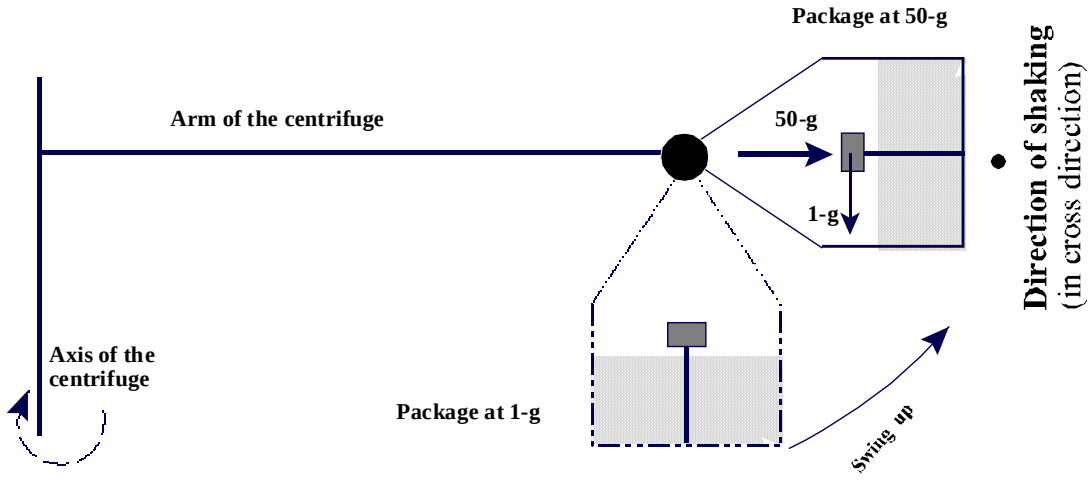

Figure 4.27: The forces that act on the model pile.

The effect of 1-g was countered in tests SB-03, SB-04 and SB-05 by fixing the bottom of the pile in a wedge at a slope 1 in 50 as shown in Figure 4.28. This corrects the imperfection in simulated gravity and imposes a purely axial load in the pile at 50-g.

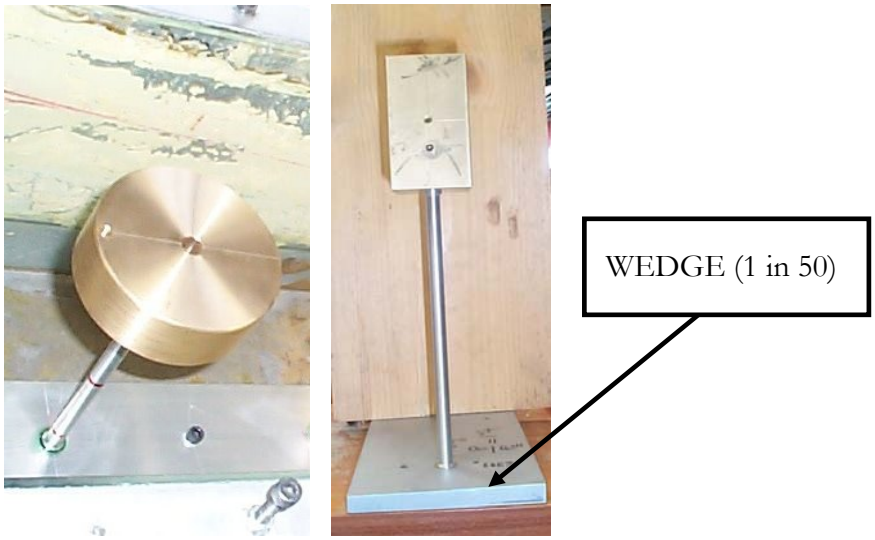

Figure 4.28: Method adopted to simulate axial load in pile and to minimise the 1-g effect

4.10.1 Decoupling effects of axial and inertia

Table 4.12 summarises the centrifuge tests stating the parameters involved. It may be noted that through the sequence of tests the loading effects mentioned in section 4.10 were successfully decoupled. In test SB-02, all three effects were present while in test SB-04 only the effects of axial load were studied.

In test SB-04, a specially designed frame was used to restrain the head mass against inertial action as shown in Figure 4.29. Thus the pile is only allowed to move in a transverse direction orthogonal to the direction of shaking. Also, while the wedge corrects the 1-g effect at 50-g, at lower g levels the load acting is still not purely axial, Figure 4.30. To avoid premature failure while the g-level is being increased, a retractable pneumatic piston was used to hold the head mass temporarily (Figure 4.31). From the figure it may be noticed that a wooden block is loosely held in between the pile head mass and the piston to increase the gap between the frame and the pile head mass. The pressure in the piston was released when the package reached 50-g and the wooden block fell in the soil while pile remained stable. Figure 4.32 explains schematically the above-mentioned working action.

Lateral shaking was then imparted to the model. Test SB-04 was repeated as SB-05, but without soil. Therefore, the various influences on pile behaviour could be distinguished.

Table 4.12: Summary of the tests

Test ID	Parameters involved in the test	Remarks
SB-02 (with soil)	1-g effect, axial load and inertial effects	Two piles failed during swing up due to 1-g effect.
SB-03 (with soil)	The effect of axial load and inertia load	1-g effect removed by wedge
SB-04 (with soil)	Only the effect of axial load	1-g and inertial effects removed
SB-05 (no soil)	Only the effect of axial load	1-g and inertial effects removed
SB-06 (with soil)	The effect of axial load and inertia	Pile-soil interaction was studied

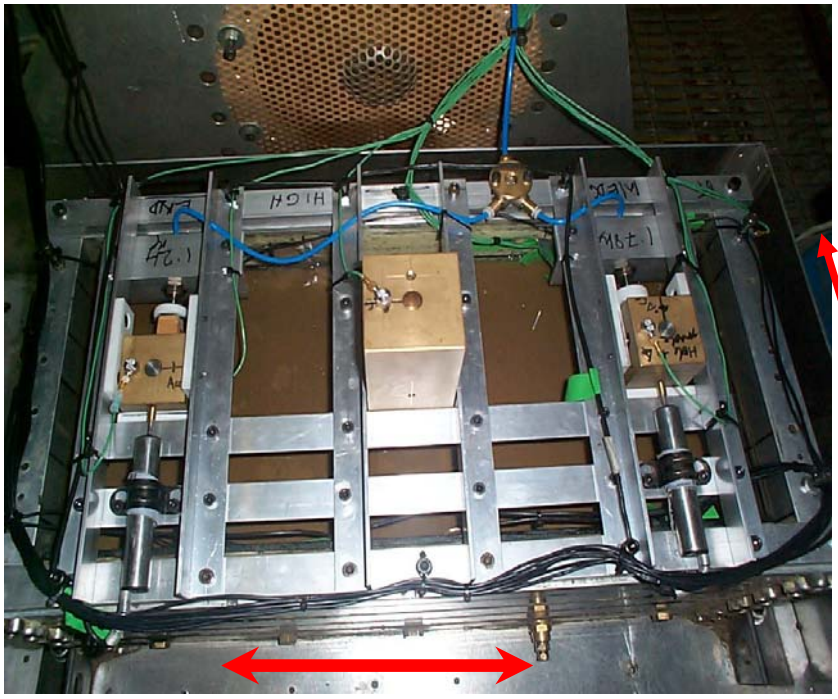

Figure 4.29: Test SB-04 with guides to hold the masses against inertia force.

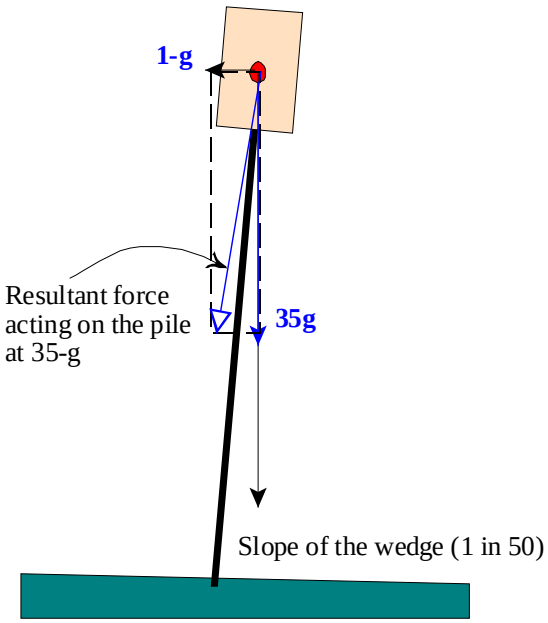

Figure 4.30: Eccentricity of load at 35g (a g-level chosen as an example and has no significance).

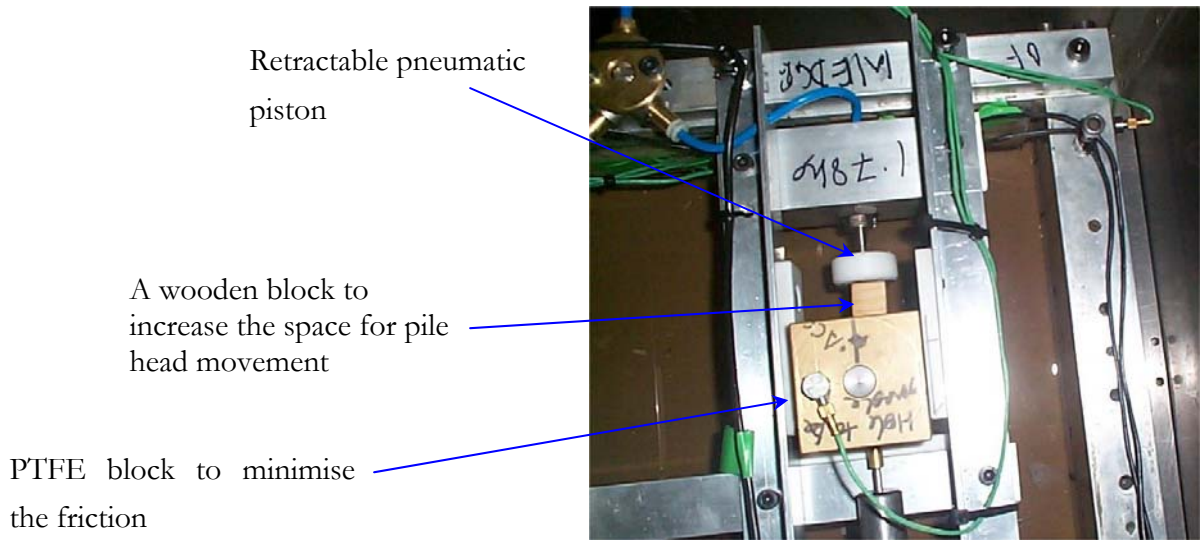

Figure 4.31: Set up to hold the pile during the swing up.

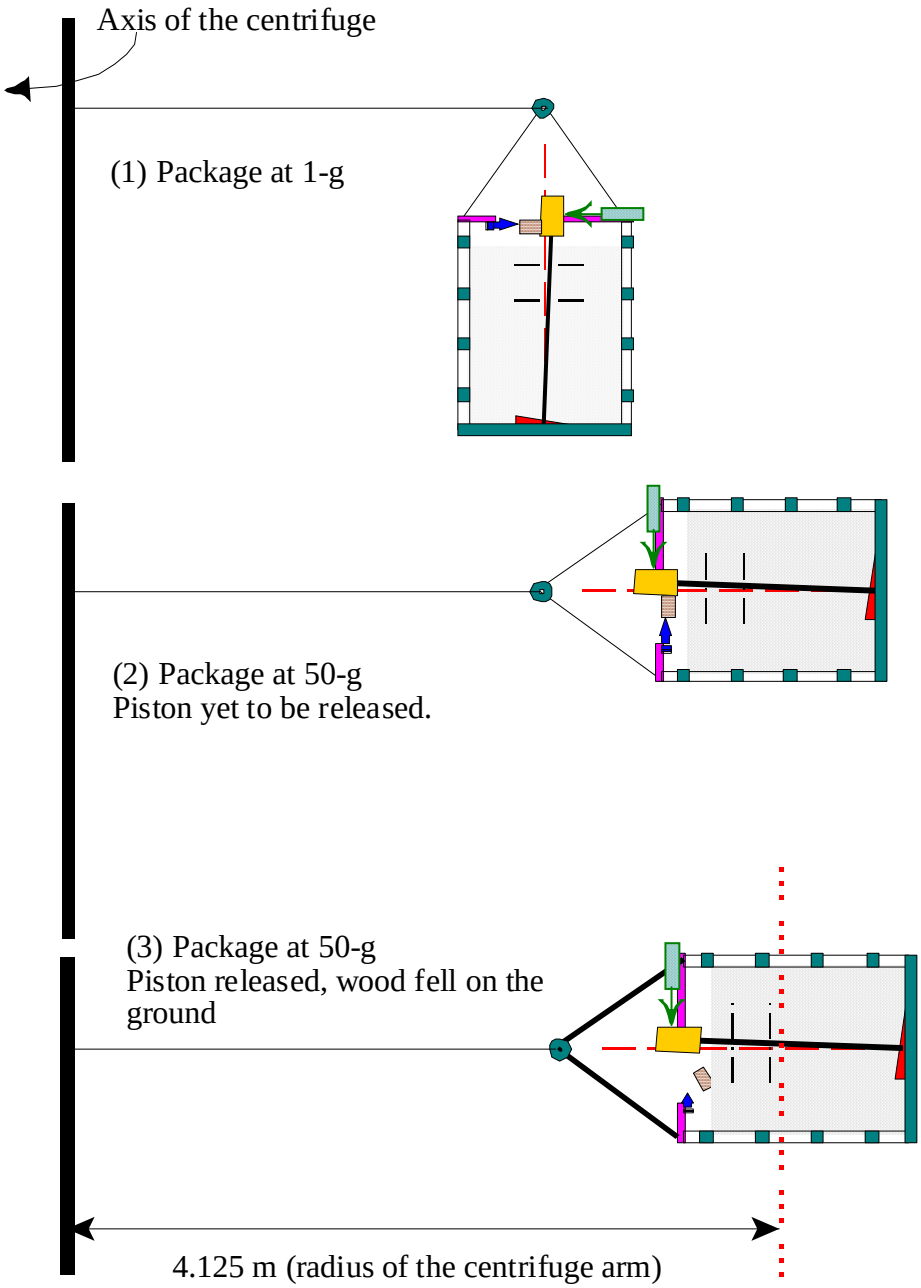

Figure 4.32: Schematic diagram showing the action of test procedure in test SB-04.

4.10.2 Investigation of pile soil interaction

Different aspects of pile soil interaction were studied in the centrifuge tests. One of the main aims of the test SB-06 was to quantify some aspects of pile movement during seismic liquefaction. A spring-loaded LVDT was held against the pile head to follow the movement of the pile head mass as shown in Figure 4.33. The force imposed by the spring was negligible. Near field pore pressures were also measured by placing the PPT's very close to the pile (Figure 4.34).

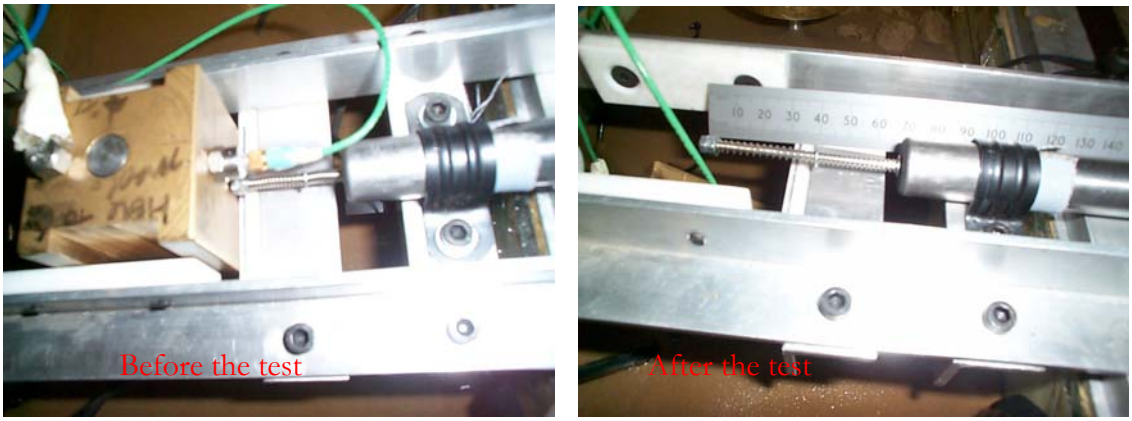

Figure 4.33: Action of spring loaded LVDT in test SB-06.

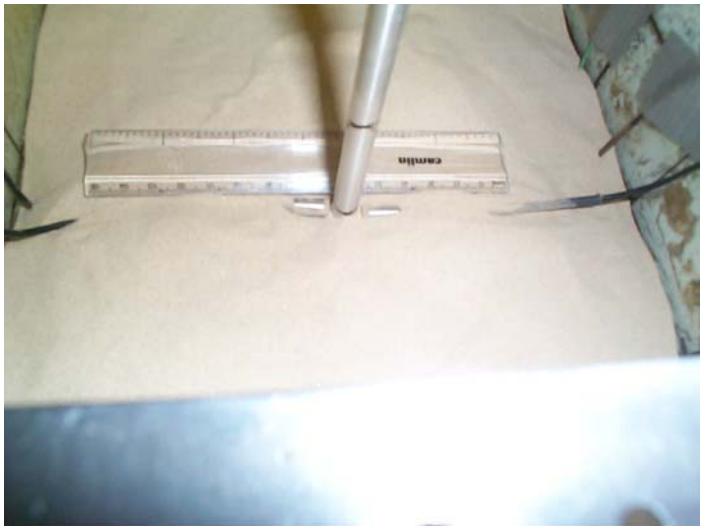

Figure 4.34: PPT's placed in near field of the pile

4.11 Summary

Dynamic centrifuge modelling has been shown to be feasible for verifying proposed mechanisms. Model composite piles (aluminium-foam) are not suitable for investigating buckling instability problems. Model dural piles were shown to be representative of a real pile and thus the results of the centrifuge tests can be used to calibrate real pile problems. Schemes used to decouple different load effects were demonstrated. In the centrifuge tests the pile installation effects were not modelled. Chapter 5 plots and analyses the results of the centrifuge tests.